Journal of Biomechanics 47 (2014) 3813–3819

Contents lists available at ScienceDirect

Journal of Biomechanics

journal homepage: www.elsevier.com/locate/jbiomech
www.JBiomech.com

Influence of tendon tears on ultrasound echo intensity in response to loading

Kayt E. Frisch [a,*], David Marcu [b], Geoffrey S. Baer [c], Darryl G. Thelen [d], Ray Vanderby [e]

[a] Department of Engineering/Dordt College/Sioux Center, Iowa, United States
[b] Sauk Prairie Memorial Hospital, Prairie du Sac, Wiscosin, United States
[c] Department of Orthopedics and Rehabilitation/University of Wisconsin, Madison, Wiscosin, United States
[d] Department of Biomedical Engineering, Department of Mechanical Engineering/University of Wisconsin, Madison, Wiscosin, United States
[e] Departments of Orthopedics and Rehabilitation and Biomedical Engineering/University of Wisconsin, Madison, Wiscosin, United States

ARTICLE INFO

Article history:
Accepted 17 October 2014

Keywords:
Tendon
Mechanics
Ultrasound
Acoustoelastic
Damage
Tear

ABSTRACT

Acoustoelastic (AE) ultrasound image analysis is a promising non-invasive approach that uses load-dependent echo intensity changes to characterize stiffness of tendinous tissue. The purpose of this study was to investigate whether AE can detect localized changes in tendon stiffness due to partial and full-thickness tendon tears. Ovine infraspinatus tendons with different levels of damage (Intact, 33%, 66% and full thickness cuts initiated on the articular and bursal sides) were cyclically loaded in a mechanical testing system while cine ultrasound images were recorded. The load-induced changes in echo intensity on the bursal and articular side of the tendon were determined. Consistent with AE theory, the undamaged tendons exhibited an increase in echo intensity with tendon loading, reflecting the strain-stiffening behavior of the tissue. In the intact condition, the articular region demonstrated a significantly greater increase in echo intensity during loading than the bursal region. Cuts initiated on the bursal side resulted in a progressive decrease in echo intensity of the adjacent tissue, likely reflecting the reduced load transmission through that region. However, image intensity information was less sensitive for identifying load transmission changes that result from partial thickness cuts initiated on the articular side. We conclude that AE approaches may be useful to quantitatively assess load-dependent changes in tendon stiffness, and that disruption of AE behavior may be indicative of substantial tendon damage.

1. Introduction

Tendon tears are often diagnosed using either B-mode ultrasound (US) or magnetic resonance (MR) imaging, and while ultrasound has an advantage of being cost-effective and readily available (Awerbuch, 2008), assessing partial thickness tendon tears in B-mode images can be difficult (Miller et al., 2002; Sipola et al., 2010; McConville and Iannotti, 1999; Teefey et al., 2000; Vlychou et al., 2009). Because the degree of partial thickness tears is a commonly used criterion for deciding between conservative and surgical treatments in the rotator cuff tendons (Flatow et al., 1997; Fukuda et al., 1996; Peterson and Altchek, 1996; Weber, 1999), there is substantial interest in quantitative ultrasound techniques that can more objectively assess the ramifications of a tear on tendon mechanical properties and function. Prior ex vivo experiments have shown that tendon tearing significantly affects deformation and strain patterns in the rotator cuff tendons (Andarawis-Puri et al., 2009; Bey et al., 2002; Mazzocca et al., 2008; Yang et al., 2009), suggesting that the tendon stiffness may also be affected.

Ultrasound has previously been used to estimate strain and stiffness in tendon by visually tracking motion of a muscle-tendon junction during loading (Farron et al., 2009; Maganaris, 2002; Reeves et al., 2009; Reeves et al., 2003; Arya and Kulig, 2010). Elastography approaches have also been used for estimating tissue strain and inferring stiffness by cross-correlating the ultrasound radiofrequency (RF) signals collected from tissue in unloaded and loaded states (Doyley et al., 2000; Kallel et al., 1996; Kallel and Bertrand, 1996; Ophir et al., 2000; Ponnekanti et al., 1992; Ponnekanti et al., 1995). Several studies have applied elastography to tendon, showing that the stiffness of tendon varies spatially within the tendon and that it is altered in damaged tissue (DeZordo et al., 2009; Spalazzi et al., 2006). More recently, shear wave elastography has shown that the speed of shear wave propagation in tendon is affected by the presence of tears (Dewall et al., 2014). These elastography-based techniques show

* Corresponding author at: Dordt College 498 4th Ave NE, Sioux Center, IA 51250. Tel. +712 722 6306; fax: +712 722 6035.
E-mail addresses: kayt.frisch@dordt.edu (K.E. Frisch), dmarcu@spmh.org (D. Marcu), baer@ortho.wisc.edu (G.S. Baer), thelen@engr.wisc.edu (D.G. Thelen), Vanderby@ortho.wisc.edu (R. Vanderby).

http://dx.doi.org/10.1016/j.jbiomech.2014.10.026
0021-9290/

promise, but stiffness inference from elastography is typically based on an assumption of tissue homogeneity, which does not reflect the anisotropic structure of tendon (Abrahams, 1967; Garcia et al., 2003; Ophir et al., 2000; Rigby et al., 1959; Szabo, 2004).

An alternative method for estimating tendon stiffness is acoustoelasticity (AE), a theory based on the principle that the acoustic properties of a material change as the material deforms (Hughes and Kelly, 1953). AE predicts that the magnitude of a reflected ultrasound wave increases as the material undergoes strain-stiffening during loading (Kobayashi and Vanderby, 2007, 2009). The relationship between the mechanical stiffness of a material and the magnitude of the reflected ultrasound wave has been described for a single RF ultrasound beam line in a deformed, nearly incompressible material (Kobayashi and Vanderby, 2007, 2009). A B-Mode image presents many RF beams as grayscale intensity values ranging from black (no reflection) to white (substantial reflection). Thus, AE predicts that the intensity (brightness) of the B-mode image will increase with increasing load, referred to herein as the acoustoelastic effect. This AE effect has been observed in both tendon and skin (Crevier-Denoix et al., 2005; Pan et al., 1998). In tendon, the echo intensity increased proportionately with tissue stress and strain in cyclically loaded intact tendon (Duenwald et al., 2010). This suggests that AE may be able to non-invasively quantify localized damage-dependent changes in tendon stiffness (Crevier-Denoix et al., 2005; Duenwald et al., 2010; Pan et al., 1998). The purpose of the present study is to use an ex vivo ovine infraspinatus tendon (IST) model to investigate how partial (PT) and full (FT) thickness tendon tears affect echo intensity change during cyclic loading. Similar to our prior studies on porcine flexor tendons (Duenwald et al., 2010), we expected that both the articular and bursal regions of the intact sheep infraspinatus tendon would exhibit an AE effect in response to cyclic loading. We further hypothesized that the echo intensity changes would diminish in tissue adjacent to a partial thickness cut. Conversely, we expected the echo intensity on the side of tendon opposite to the cut to continue increasing proportionally with stretch. We also compared load-dependent changes in echo intensity between the bursal and articular sides of the intact tendon, since prior studies suggest varying stiffness and non-uniform deformation across the tendon thickness (Bey et al., 2002; Nakajima et al., 1994; Reilly et al., 2003).

2. Methods

2.1. Specimen preparation

Infraspinatus tendons (IST) were excised bilaterally from seventeen skeletally mature female sheep (being euthanized for an unrelated study) immediately after sacrifice. The surrounding tissue was carefully removed, leaving only the humerus, the IST and the infraspinatus muscle intact. The specimens were stored at -80 °C until testing. Specimens were kept moist with physiologic buffered saline (PBS) throughout preparation and storage. Immediately prior to mechanical testing, the infraspinatus muscle was removed from the tendon. The long bone portion of the humerus was also removed, while leaving the tendon insertion site intact. A hole was then drilled in the center of the humeral head to facilitate gripping for the mechanical testing. A total of 17 IST tendons from nine sheep were used in the study (one tendon was excluded due to damage during harvesting).

2.2. Mechanical testing

Mechanical testing was performed using a servo-hydraulic mechanical test system (Bionix 858, MTS, Minneapolis, MN, USA) with the tendon mounted in a custom bath (Fig. 1). The humerus was mounted on an L-shaped bracket made of 1/2 in. thick steel plate, by placing a threaded post through the hole in the humeral head and tightening it in place using a nut and washer. Rotation of the bone was prevented by the metal track spikes that were placed in a grid on the vertical surface of the bracket. The bracket was attached to the bath with a large washer and a wing nut. The soft tissue end of the tendon was secured in a textured sandwich grip attached to the load cell. Specimens were mounted at approximately 15° of glenohumeral abduction. Displacement between the grips was controlled by the servo-hydraulic testing system and the resulting load was measured with a 500 lb load cell (Eaton Coporation, Clevland, OH, USA). Once secured, tendons were pre-loaded to 2 N to remove slack. Following preloading, the grip-to-grip length of the tendon was measured using a digital calipers and tendons were preconditioned at 1 Hz for 10 cycles to 2% strain (based on the measured length). Following preconditioning and all subsequent tests, specimens were allowed to rest for 500 seconds to ensure adequate recovery between tests. For mechanical testing a cyclic load (frequency = 0.5 Hz) was applied for 10 cycles to 4% peak strain. To avoid strain history-dependent effects, only the last three cycles were analyzed.

2.3. Defect creation

Defects mimicking partial and full-thickness avulsion tears were created near the tendon-bone insertion using a razor blade on a custom-designed handle. All tendons in this study had similar thickness, so defects were created using a constant depth. After testing the intact tendons to obtain a set of baseline mechanical and ultrasonic measurements, the experimental group of tendons received a 14[mm] wide by 3[mm] deep defect (approximately 33% of thickness of the insertion) from either the bursal ($n=9$) or articular ($n=8$) side of the tendon (Fig. 2) to simulate a small partial tear. After repeating the mechanical testing protocol, the defect was deepened to 6[mm] (approximately 66% of the insertion

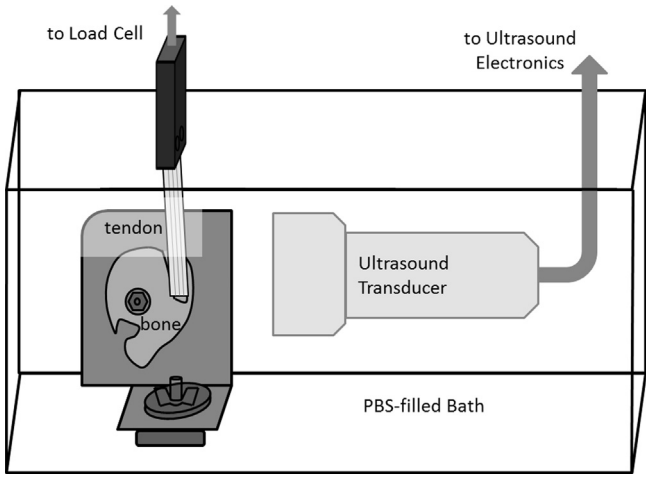

Fig. 1. Tendon test setup with ultrasound. Sheep infraspinatus bone-tendon units were mounted in a custom bath affixed to a servo-hydraulic machine for mechanical testing. An ultrasound transducer was placed in the bath to record cine B-Mode images during cyclic axial loading.

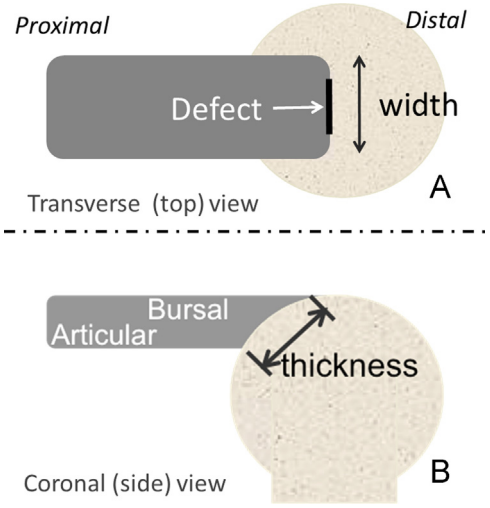

Fig. 2. The width and thickness designations used for tendon defect creation. (A) Side view of the tendon, indicating bursal and articular sides and the thickness across the footprint. (B) Top view of the tendon showing the width of the tendon and the location of the defect.

thickness) and tested before finally creating a full thickness defect, such that the tendon was only attached by residual tissue segments on either side of the defect.

2.4. Ultrasound imaging

Cine ultrasound was recorded using a GE LOGIQe ultrasound machine equipped with a 12 L-RS Linear Array Transducer (General Electric, Fairfield, CT, USA). The ultrasound transducer was placed in the ultrasound bath 2. 5 cm from the tendon (Fig. 1) and attached to the wall of the bath using a custom-built clamp. The transducer was aligned with long (azimuthal) axis of the parallel to the long (loading) axis of the tendon and centered over the location where the defect was to be made. Cine B-mode ultrasound video (frequency: 12 MHz, gain: 18, frame rate: 20 fps) was recorded for the last three steady-state cycles of mechanical testing. Images were manually synchronized with the mechanical loading data.

2.5. Image analysis

On the first image of the unloaded tendon, a region of interest (ROI) was manually defined by selecting vertices along the articular and bursal edges of the tendon. Longitudinally, the ROI extended from the bony insertion to the most proximal region that remained within the image window at the maximum applied displacement. The ROI was then divided into two equal width sub regions (articular and bursal) for analysis (Fig. 3).

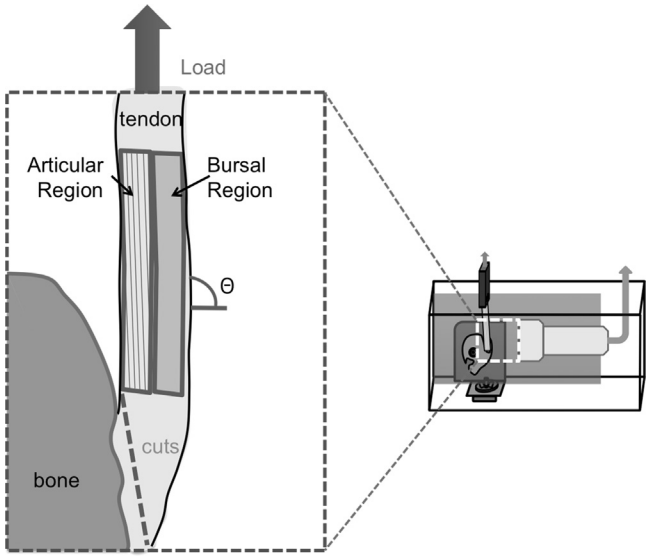

Fig. 3. The tendon was divided into two regions (bursal and articular) for image analysis. Tendon defects were created by cutting the tendon near its insertion onto the humerus. The angle of the tendon loading direction relative to the transducer, θ, was measured as indicated. The inset shows the orientation of the ultrasound image relative to the test setup.

To ensure that the same region of tendon was being evaluated in each frame, the motion of the region was tracked from frame to frame using a digital image correlation technique adapted especially for ultrasound images (EchoMetrix, Madison, WI, USA). This code tracks the apparent movement of the "speckles" present in B-mode ultrasound images and uses a summed-squared difference metric to estimate movement of speckles between ROI frames, as described previously by Duenwald, et al. (Duenwald et al., 2010). The average grayscale echo intensity inside the ROI, I, was calculated for every tracked frame in each trial and normalized relative to intensity in the last unloaded frame for that trial, I_0, as is traditionally done with strain:

$$\Delta I = \frac{I - I_0}{I_0} \times 100\%$$

The echo intensity change for each specimen was evaluated at 3.5% applied strain (as measured by the mechanical testing system) to facilitate standard comparisons between conditions. We performed retrospective analysis to determine the sensitivity of reflected wave intensity to transducer orientation. To do this, the angle (θ) of the tendon fascicles relative to the transducer (Fig. 3) was measured using Image J (U. S. National Institutes of Health, Bethesda, Maryland, USA).

2.6. Statistics

A mixed effects ANOVA with cut location (bursal, articular) and cut depth (0%, 33%, 66% and full thickness) as fixed effects and specimen as a random effect was performed on the intensity outcome measures to examine the differences in each measure based on category and classification. To standardize the measures for each specimen relative to the fully intact condition, the post hoc analyses presented are based on the paired differences from intact to the various depths of cut. Post-hoc testing between the different cut locations at a given depth (e. g. small articular vs. small bursal at 33% cut) was performed using Tukey HSD tests. Post-hoc testing between the different cut severity for a given cut size and location (e.g. intensity at 33% cut vs. 66% cut for large bursal) was also performed using Tukey HSD tests. Differences between each defect severity and intact for a given cut location (e.g. change in intensity at 33% relative to intact for bursal) were assessed with Holm adjusted p-values from paired T-tests. Significance for all tests was set at $p=0.05$. If the p-value was less than 0.1 the difference was considered a noticeable trend.

3. Results

For the intact tendons, the average ultrasound grayscale echo intensity varied cyclically in response to cyclic loading (Fig 4A). However once a defect was created, a substantial reduction in echo intensity relative to the intact case was observed (Fig. 4C, D).

In the intact case there was a significant ($p=0.027$) difference in echo intensity change between the bursal and articular regions, with the articular region having a higher average echo intensity change (12.4 ± 1.7 [% of unloaded] compared to 9.6 ± 2.3 [% of unloaded] for the bursal region) at 3.5% applied strain (Fig. 5).

Echo intensity at 3.5% applied strain was more affected by partial-thickness defects created from the bursal side of the

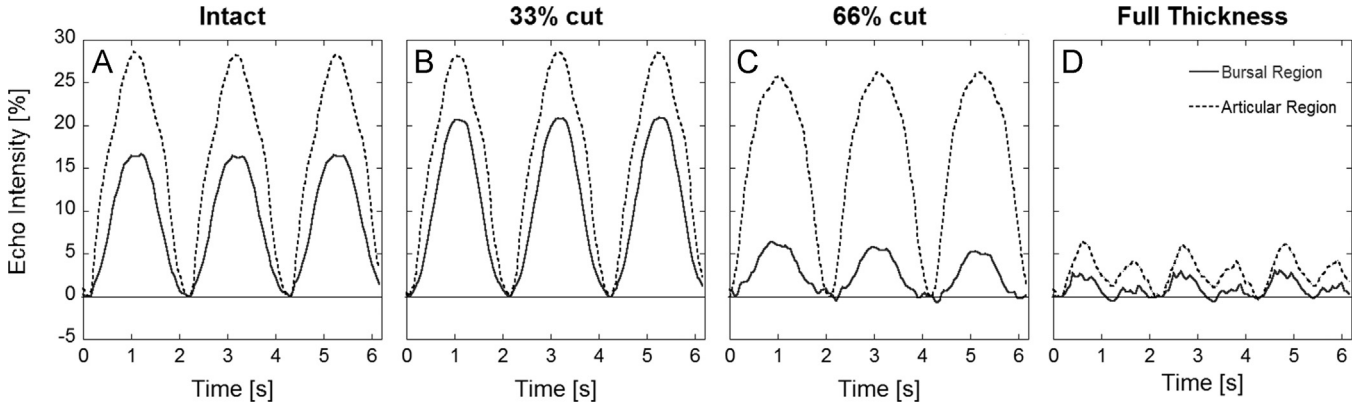

Fig. 4. Change in image echo intensity over time during cyclic loading. Shown are mean regional change in echo intensity normalized to the first unloaded frame for a single specimen during the 3 testing cycles for (A) intact tendon, (B) 33% of the thickness cut, (C) 66% of the thickness cut and (D) the full thickness cut. Note that the intact echo intensity changes cyclically in response to the applied cyclic displacement. When the cut depth reaches 66%, the bursal region (the side cut on this specimen) has a diminished echo response and both regions have a diminished response for the full thickness cut.

tendon (Fig. 6, Table 1). When the full thickness of the tendon fibers in view of the transducer were cut, the AE effects in the bursal region decreased significantly ($p=0.008$) from 11.2 ± 4.2 [% of unloaded] (intact) to 2.0 ± 2.7 [% of unloaded] (full thickness) for the bursal sided defect and decreased significantly ($p=0.01$) from 7.9 ± 1.7 [% of unloaded] (intact) to 1.4 ± 1.7 [% of unloaded] (full thickness) for the articular sided defect. The bursal sided defect also caused a significant ($p=0.001$) decrease from 12.8 ± 3.0 [% of unloaded] (intact) to 2.9 ± 2.1 [% of unloaded] (full thickness) in the articular region of the tendon.

For partial thickness cuts, the bursal region was most sensitive to bursal defects, with a significant reduction in echo intensity from the intact group observed for all three depths. However, the intensity change relative to the intact did not vary significantly between regions for cuts initiated on the articular side (Fig. 7, Table 2).

The angle between the transducer and the tendon did have an effect on the echo intensity (Fig. 8), with less intensity change observed when the fibers were more perpendicular to the transducer beam direction.

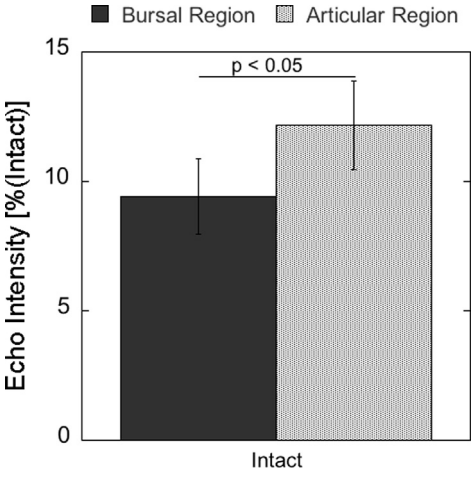

Fig. 5. Echo intensity change in the bursal and articular regions for intact tendon. For intact tendon, the bursal region has a significantly lower normalized (relative to the value for the region in the unloaded frame) average echo intensity change than the articular region when 3.5% strain has been applied. According to AE theory, such a difference could arise from stiffness difference between the two sides of the tendon.

Table 1
P-values for strain comparisons by cut group and region. Bursal region: (A) Large Bursal-sided Group. (B) Large Articular-sided Group. Articular region: (C) Large Bursal-sided Group. (D) Large Articular-sided Group. For each cut condition relative to intact p-values were calculated using a Holm adjusted Bonferroni comparison to account for the multiple comparisons. For the comparisons between other cut conditions adjusted p-values were calculated using a Tukey HSD test.

(A) Bursal region (Bursal defect)

	Intact	*33%*	*66%*	*Full*
Intact	–	**0.008**	**0.006**	**0.008**
33%		–	0.711	0.066
66%			–	0.278
Full				–

(B) Bursal region (Articular defect)

	Intact	*33%*	*66%*	*Full*
Intact	–	0.821	0.994	**0.01**
33%		–	0.949	**0.003**
66%			–	**0.001**
Full				–

0.5

(C) Articular region (Bursal defect)

	Intact	*33%*	*66%*	*Full*
Intact	–	0.335	0.401	**0.001**
33%		–	0.989	0.125
66%			–	0.096
Full				–

(D) Articular region (Articular defect)

	Intact	*33%*	*66%*	*Full*
Intact	–	0.948	0.89	0.067
33%		–	0.821	0.066
66%			–	**0.019**
Full				–

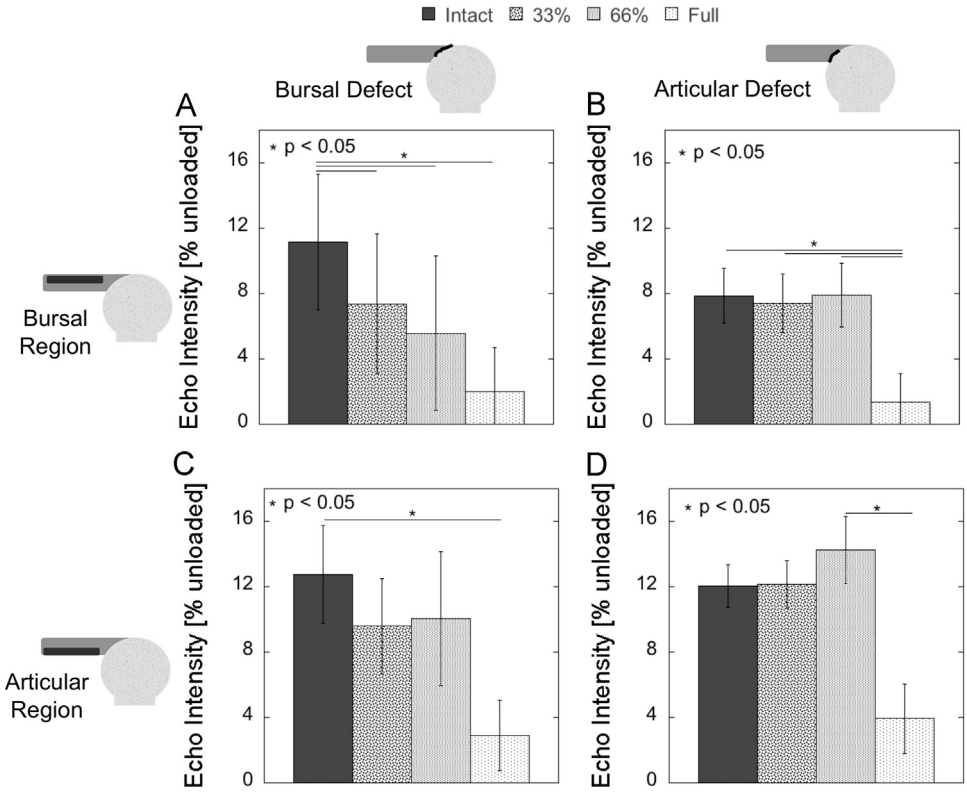

Fig. 6. Echo intensity (relative to unloaded) at 3.5% applied strain for: (A) the bursal region/bursal defect, (B) the bursal region/articular defect, (C) the articular region/bursal defect, and (D) the articular region/articular defect. Note that (A) decreases as the cut increases and that (B) and (C) do not change until the full thickness defect. (D) was expected to be similar to (A) but it is not. In all cases the only statistically significant case is the full thickness cut. Bars represent standard error.

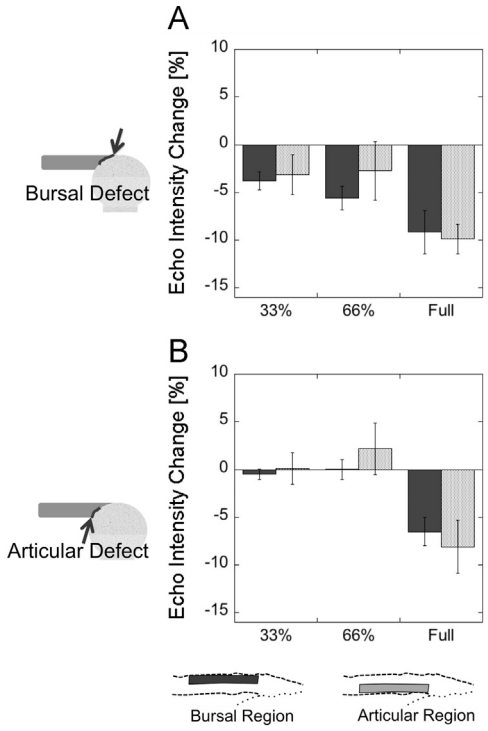

Fig. 7. Change in echo intensity (relative to intact) at 3.5% applied strain comparing the change in the bursal region with the change in the articular region for (A) the bursal defect group and (B) the articular defect group. There are no statistically significant differences between the regions for any of the cut groups.

Table 2
P-values for comparisons between the bursal and articular regions for each defect group. The change from intact for the two regions were not significantly different ($p < 0.05$) for either defect at any depth of cut. For the different cut conditions values were calculated using a Holm adjusted Bonferroni comparison to account for the multiple comparisons.

	33% Cut	66% Cut	Full Cut
Bursal defect	0.75	0.53	0.782
Articular defect	0.711	0.463	1

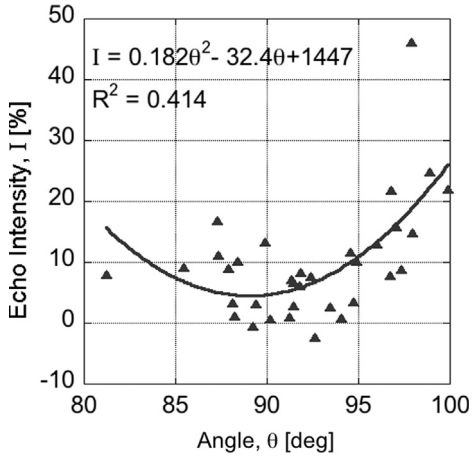

Fig. 8. The echo intensity (relative to unloaded) at 3.5% applied strain for all intact tendons. There is a tendency ($R^2 = 0.414$) toward an angle dependence that is approximately symmetric around 90°. If the two apparent outliers are removed the correlation becomes $R^2 = 0.549$.

4. Discussion

The purpose of this study was to investigate the use of ultrasound AE for quantifying regional stiffness differences due to tendon tears. We first demonstrated that echo intensity varies systematically with loading in the sheep infraspinatus tendon, an effect consistent with acoustoelastic theory (Duenwald et al., 2010; Kobayashi and Vanderby, 2007, 2009). We then introduced tears on the bursal and articular sides of tendon and assessed how the reflected ultrasound signal changed during loading. The data demonstrate that this load-dependent echo intensity varies with damage, and is most substantially disrupted in tendons that have suffered a full-thickness tear.

Based on AE theory and previous experiments with porcine flexor tendons, we expected that the intensity of the ultrasound signal reflected from cyclically loaded tendon will vary cyclically, due to the strain-stiffening behavior of tendinous tissue. The anticipated cyclic behavior was observed, as the intact sheep infraspinatus tendon exhibited cyclic echo intensity variations in both the bursal and articular regions (Fig. 4) that closely corresponded to the applied stresses, following patterns previously observed in porcine flexor tendon. The results also showed inter- and intra-trial repeatability similar to those previously reported (Duenwald et al. 2010).

We had hypothesized we would see a decrease in echo intensity in the tissue adjacent to a tendon tear (Fig 6A & D). This hypothesis was supported with tissue on the side of the cut tending to show a decrease in echo intensity change for the bursal-sided defects (Fig. 4C & D). Mechanically, this would be expected since the cut tendon fibers will no longer experience tension, and hence will not exhibit strain-stiffening behavior. We also expected that the magnitude of intensity decrease would relate to the depth of cut (Fig 6A & D). This gradual decrease in echo intensity would occur because more of the fibers in the imaging region were becoming unloaded with each successive cut. We observed that in general the bursal region of the tendon behaved as expected for the bursal-sided defect, with the average echo intensity at 3.5% applied strain dropping for each successive cut. However due to variability between specimens, the echo intensity changes on the bursal side were only significant relative to the intact case (Fig 6A). Contrary to our hypothesis, the articular side defect did not result in a systematic drop in echo intensity until the depth of cut was completely though the thickness of the tendon (Fig. 6 D). One potential explanation for these results can be found in reports that the articular and bursal sides of the tendon do not share the load equally in an intact tendon (Bey et al., 2002; Nakajima et al., 1994; Reilly et al., 2003). If the articular side carried proportionally less load we would expect the intensity change to be lower after partial cuts on the articular side.

By extension, we hypothesized that the echo intensity would continue to change cyclically in the region on the opposite side from the cut (Fig. 6 B & C). We observed that the cyclic behavior remained the same after cutting and that the intensity of the reflected signal showed no significant change in the intact region of the tendon (Fig. 7, Table 2). Engineering mechanics predicts that if the displacement is controlled, the load would decrease proportionally with the decreasing area, maintaining a constant stress in the tissue, which means that the stiffness of the tissue will remain constant even though the load decreases. Since AE theory predicts that the intensity of the reflected ultrasound signal depends on the stiffness of the reflecting tissue (Kobayashi and Vanderby, 2007, 2009), we would then expect that the intensity of the reflected signal would remain unchanged.

Finally we compare AE effects between the bursal and articular regions of the intact tendon. Studies on human supraspinatus tendon indicate that the bursal and articular layers demonstrate different mechanical stiffnesses, and since the sheep infraspinatus tendon fills a similar role in the sheep we would expect to see

comparable differences in stiffness for the IST (Coleman et al., 2003; Lee et al., 2000; Nakajima et al., 1994). If this mechanical difference were true, we would expect that bursal side of the intact sheep IST to be stiffer than the articular side, and thus would reflect proportionally more of the ultrasound signal. Unexpectedly, we found that the bursal side of the tendon experienced significantly lower echo intensity change than the articular side (Fig. 5). In humans, it is believed that the bursal side of the infraspinatus tendon is stiffer and carries greater load, and thus could be expected to undergo greater intensity change with stretch (Coleman et al., 2003; Lee et al., 2000; Nakajima et al., 1994). At this point, it is unclear whether our results reflect unique behavior of the sheep infraspinatus tendon, preferential loading of the articular side of the tendon due to our experimental setup, or a transducer-fiber alignment effect. Further studies will be required to delineate which of these factors gives rise to the echo intensity variation across the tendon.

This study has several limitations. First, our in vitro methods created an idealized model. We utilized healthy sheep infraspinatus tendons isolated from the surrounding tissues and cut them to study the effects of partial and full thickness tears on the acoustoelastic effect. In an in vivo situation tearing would likely be accompanied by inflammation and possibly fraying at the damaged end, neither of which can be simulated using the present model. Second, the magnitude of echo intensity change is dependent on the angle of the ultrasound transducer relative to the tendon (Fig. 8) as well as positioning of the region of interest. The potential problems associated with transducer orientation during in vivo tendon loading were not addressed. Additionally, cutting the tendon may enable greater out of plane motion due to the fibers no longer being taut. This change in fiber orientation may have influenced the ultrasound image intensity as the tissue moves in and out of the image window. Third, in vivo tissue will be constrained more fully, which may affect the echo intensity changes described herein. Based on these findings, understanding the effects of load-dependent changes in collagen fiber orientations and positioning on reflected sound waves is important to progress acoustoelastic analysis techniques as a quantitative imaging tool for assessing tendon damage.

In conclusion, we have shown that the load-dependent image intensity changes previously observed in the porcine flexor tendon (Duenwald et al., 2010) is also present in the sheep infraspinatus tendon. We also showed that these acoustoelastic effects were significantly diminished when all of the tendon fibers in view of the transducer were cut. However, image intensity information was less sensitive for identifying stiffness changes that result from partial thickness cuts. We also note that intensity information is sensitive to transducer orientation relative to the tendon. Thus, an AE approach may be useful to quantitatively assess changes in tendon stiffness arising from substantial tendon damage, but further research is required in order to establish whether it can be useful for measuring partial tendon tears.

Conflict of interest statement

Ray Vanderby holds patents on parts of acoustoelastic theory and is part owner of EchoMetrix LLC, a company commercializing some of these applications. The other authors have no conflict of interest to declare.

Acknowledgments

Contributions by Ellen Leiferman (specimen collection), Ron McCabe (mechanical testing set-up design and fabrication), Scott Hetzel (statistics), Steve Jackson (programming), and the UW Orthopedics Resident Research Program (funding) are gratefully acknowledged. Research reported in this publication was supported by the National Institute of Arthritis and Musculoskeletal and Skin Diseases of the National Institutes of Health under Award Number AR059916 and AR56201. The content is solely the responsibility of the authors and does not necessarily represent the official views of the National Institutes of Health.

References

Abrahams, M.,, 1967. Mechanical behaviour of tendon in vitro. A preliminary report. Med. Biol. Eng. *5* (5), 433–443.

Andarawis-Puri, N., Ricchetti, E.T., Soslowsky, L.J.,, 2009. Rotator cuff tendon strain correlates with tear propagation. J. Biomech. *42* (2), 158–163. http://dx.doi.org/10.1016/j.jbiomech.2008.10.020.

Arya, S., Kulig, K.,, 2010. Tendinopathy alters mechanical and material properties of the achilles tendon. *J. Appl. Physiol.* (*Bethesda, Md.: 1985*) *108* (3), 670–675. http://dx.doi.org/10.1152/japplphysiol.00259.2009.

Awerbuch, M.S.,, 2008. The clinical utility of ultrasonography for rotator cuff disease, shoulder impingement syndrome and subacromial bursitis. Med. J. Australia *188* (1), 50–53.

Bey, M.J., Song, H.K., Wehrli, F.W., Soslowsky, L.J.,, 2002. Intratendinous strain fields of the intact supraspinatus tendon: the effect of glenohumeral joint position and tendon region. J. Orthopaed. Res. *20* (4), 869–874. http://dx.doi.org/10.1016/S0736-0266(01)00177-2.

Coleman, S.H., Fealy, S., Ehteshami, J.R., MacGillivray, J.D., Altchek, D.W., Warren, R.F., Turner, A.S.,, 2003. Chronic rotator cuff injury and repair model in sheep. J. Bone Joint Surg. Am. *85-A* (12), 2391–2402.

Crevier-Denoix, N., Ruel, Y., Dardillat, C., Jerbi, H., Sanaa, M., Collobert-Laugier, C., Pourcelot, P.,, 2005. Correlations between mean echogenicity and material properties of normal and diseased equine superficial digital flexor tendons: an in vitro segmental approach. J. Biomech. *38* (11), 2212–2220. http://dx.doi.org/10.1016/j.jbiomech.2004.09.026.

Dewall, R.J., Jiang, J., Wilson, J.J., Lee, K.S.,, 2014. Visualizing tendon elasticity in an ex vivo partial tear model. Ultrasound Med. Biol. *40* (1), 158–167. http://dx.doi.org/10.1016/j.ultrasmedbio.2013.08.022.

DeZordo, T., Lill, S.R., Fink, C., Feuchtner, G.M., Jaschke, W., Bellmann-Weiler, R., Klauser, A.S.,, 2009. Real-time sonoelastography of lateral epicondylitis: comparison of findings between patients and healthy volunteers. AJR Am. J. Roentgenol. *193* (1), 180–185. http://dx.doi.org/10.2214/AJR.08.2020.

Doyley, M.M., Meaney, P.M., Bamber, J.C.,, 2000. Evaluation of an iterative reconstruction method for quantitative elastography. Phys. Med. Biol. *45* (6), 1521–1540.

Duenwald, S., Kobayashi, H., Frisch, K., Lakes, R., Vanderby, R.,, 2010. Ultrasound echo is related to stress and strain in tendon. J. Biomech. , http://dx.doi.org/10.1016/j.jbiomech.2010.09.033.

Farron, J., Varghese, T., Thelen, D.G.,, 2009. Measurement of tendon strain during muscle twitch contractions using ultrasound elastography. IEEE T. Ultrason. Ferr. *56* (1), 27–35. http://dx.doi.org/10.1109/TUFFC.2009.1002.

Flatow, E.L., Altchek, D.W., Gartsman, G.M., Iannotti, J.P., Miniaci, A., Pollock, R.G., Warner, J.J.,, 1997. The rotator cuff. Commentary. Orthop. Clin. N. Am. *28* (2), 277–294.

Fukuda, H., Hamada, K., Nakajima, T., Yamada, N., Tomonaga, A., Goto, M.,, 1996. Partial-thickness tears of the rotator cuff. A clinicopathological review based on 66 surgically verified cases. Int. Orthop. *20* (4), 257–265.

Garcia, T., Hornof, W.J., Insana, M.F.,, 2003. On the ultrasonic properties of tendon. Ultrasound Med. Biol. *29* (12), 1787–1797.

Hughes, D.S., Kelly, J.L.,, 1953. Second-order elastic deformation of solids. Phys. Rev. *92* (5), 1145. http://dx.doi.org/10.1103/PhysRev.92.1145.

Kallel, F., Bertrand, M.,, 1996. Tissue elasticity reconstruction using linear perturbation method. IEEE T. Med. Imaging *15* (3), 299–313. http://dx.doi.org/10.1109/42.500139.

Kallel, F., Bertrand, M., Ophir, J.,, 1996. Fundamental limitations on the contrast-transfer efficiency in elastography: an analytic study. Ultrasound Med. Biol. *22* (4), 463–470.

Kobayashi, H., Vanderby, R.,, 2007. Acoustoelastic analysis of reflected waves in nearly incompressible, hyper-elastic materials: forward and inverse problems. J. Acoust. Soc. Am. *121*, 879.

Kobayashi, H., Vanderby, R.,, 2009. New strain energy function for acoustoelastic analysis of dilatational waves in nearly incompressible, hyper-elastic materials. J. Appl. Mech. *72*, 843.

Lee, S.B., Nakajima, T., Luo, Z.P., Zobitz, M.E., Chang, Y.W., An, K.N.,, 2000. The bursal and articular sides of the supraspinatus tendon have a different compressive stiffness. Clin. Biomech. (Bristol, Avon) *15* (4), 241–247.

Maganaris, C.N.,, 2002. Tensile properties of in vivo human tendinous tissue. J. Biomech. *35* (8), 1019–1027.

Mazzocca, A.D., Rincon, L.M., O'Connor, R.W., Obopilwe, E., Andersen, M., Geaney, L., Arciero, R.A., 2008. Intra-articular partial-thickness rotator cuff tears: analysis of injured and repaired strain behavior. Am. J. Sport. Med. *36* (1), 110–116. http://dx.doi.org/10.1177/0363546507307502.

McConville, O.R., Iannotti, J.P.,, 1999. Partial-thickness tears of the rotator cuff: evaluation and management. *J. Am. Acad. Orthopaed. Surgeons 7* (1), 32–43.
Miller, S.L., Hazrati, Y., Cornwall, R., Hayes, P., Gothelf, T., Gladstone, J.L., Flatow, E.L.,, 2002. Failed surgical management of partial thickness rotator cuff tears. Orthopedics *25* (11), 1255–1257.
Nakajima, T., Rokuuma, N., Hamada, K., Tomatsu, T., Fukuda, H.,, 1994. Histologic and biomechanical characteristics of the supraspinatus tendon: reference to rotator cuff tearing. *J. Shoulder Elb. Surg. / Am. Shoulder Elb. Surgeons…* [et al.] *3* (2), 79–87. http://dx.doi.org/10.1016/S1058-2746(09)80114-6.
Ophir, J., Garra, B., Kallel, F., Konofagou, E., Krouskop, T., Righetti, R., Varghese, T.,, 2000. Elastographic imaging. Ultrasound Med. Biol. *26* (*Suppl 1*), S23–S29.
Pan, L., Zan, L., Foster, F.S.,, 1998. Ultrasonic and viscoelastic properties of skin under transverse mechanical stress in vitro. Ultrasound Med. Biol. *24* (7), 995–1007.
Peterson, C.A., Altchek, D.W.,, 1996. Arthroscopic treatment of rotator cuff disorders. Clin. Sport Med. *15* (4), 715–736.
Ponnekanti, H., Ophir, J., Cespedes, I.,, 1992. Axial stress distributions between coaxial compressors in elastography: an analytical model. Ultrasound Med. Biol. *18* (8), 667–673.
Ponnekanti, H., Ophir, J., Huang, Y., Céspedes, I.,, 1995. Fundamental mechanical limitations on the visualization of elasticity contrast in elastography. Ultrasound Med. Biol. *21* (4), 533–543.
Reeves, N.D., Maganaris, C.N., Maffulli, N., Rittweger, J.,, 2009. Human patellar tendon stiffness is restored following graft harvest for anterior cruciate ligament surgery. J Biomech. *42* (7), 797–803. http://dx.doi.org/10.1016/j.jbiomech.2009.01.030.
Reeves, N.D., Narici, M.V., Maganaris, C.N.,, 2003. Strength training alters the viscoelastic properties of tendons in elderly humans. Muscle Nerve *28* (1), 74–81. http://dx.doi.org/10.1002/mus.10392.
Reilly, P., Amis, A.A., Wallace, A.L., Emery, R.J.H.,, 2003. Mechanical factors in the initiation and propagation of tears of the rotator cuff. Quantification of strains of the supraspinatus tendon in vitro. *J. Bone Joint Surg. Brit. 85* (4), 594–599.
Rigby, B.J., Hirai, N., Spikes, J.D., Eyring, H.,, 1959. The mechanical properties of rat tail tendon. J. Gen. Physiol. *43* (2), 265–283.
Sipola, P., Niemitukia, L., Kröger, H., Höfling, I., Väätäinen, U.,, 2010. Detection and quantification of rotator cuff tears with ultrasonography and magnetic resonance imaging – a prospective study in 77 consecutive patients with a surgical reference. Ultrasound Med. Biol. *36* (12), 1981–1989. http://dx.doi.org/10.1016/j.ultrasmedbio.2010.09.001.
Spalazzi, J.P., Gallina, J., Fung-Kee-Fung, S.D., Konofagou, E.E., Lu, H.H.,, 2006. Elastographic imaging of strain distribution in the anterior cruciate ligament and at the ligament-bone insertions. J. Orthopaed. Res.: Official Publ. Orthopaed. Res. Soc. *24* (10), 2001–2010. http://dx.doi.org/10.1002/jor.20260.
Szabo, T.,, 2004. *Diagnostic Ultrasound Imaging: Inside Out*,, first ed. Academic Press.
Teefey, S.A., Hasan, S.A., Middleton, W.D., Patel, M., Wright, R.W., Yamaguchi, K.,, 2000. Ultrasonography of the rotator cuff. A comparison of ultrasonographic and arthroscopic findings in one hundred consecutive cases. *J Bone Joint Surg. Am. 82* (4), 498–504.
Vlychou, M., Dailiana, Z., Fotiadou, A., Papanagiotou, M., Fezoulidis, I.V., Malizos, K.,, 2009. Symptomatic partial rotator cuff tears: diagnostic performance of ultrasound and magnetic resonance imaging with surgical correlation. Acta Radiol. (Stockholm, Sweden: 1987) *50* (1), 101–105. http://dx.doi.org/10.1080/02841850802600764.
Weber, S.C.,, 1999. Arthroscopic debridement and acromioplasty versus mini-open repair in the treatment of significant partial-thickness rotator cuff tears. Arthroscopy: The J. Arthroscopic Related Surg.: Official Publ. Arthroscopy Assoc. N. Am. Int. Arthroscopy Assoc. *15* (2), 126–131. http://dx.doi.org/10.1053/ar.1999.v15.0150121.
Yang, S., Park, H.-S., Flores, S., Levin, S.D., Makhsous, M., Lin, F., Zhang, L.-Q.,, 2009. Biomechanical analysis of bursal-sided partial thickness rotator cuff tears. J. Shoulder Elb. Surg. / Am. Shoulder . Elb. Surg. *18* (3), 379–385. http://dx.doi.org/10.1016/j.jse.2008.12.011.